Photosynthesis Research **64:** 41–52, 2000.

Regular paper

Characterization of a symmetrized mutant RC with 42 residues from the Q_A site replacing residues in the Q_B site

Jiali Li[3], W.J. Coleman[2], D.C. Youvan[2] & M. R. Gunner[1,*]
[1]*Department of Physics, Rm. J419, City College of New York, 138th St. and Convent Ave., New York, NY 10031, USA;* [2]*KAIROS Scientific Inc. Bldg. 62, 3350 Scott Blvd., Santa Clara, CA 95054 USA;* [3]*Current address: Physics Department, Harvard University, 17 Oxford Street Jefferson Labs, Cambridge, MA 02138, USA;* [*]*Author for correspondence (e-mail: gunner@sci.ccny.cuny.edu; fax: +1-212-650-6940)*

Received 19 November 1999; accepted in revised form 27 March 2000

Key words: binding, electron transfer, quinone, reaction center

Abstract

The electron transfer reactions involving Q_A and Q_B were investigated in *Rb. capsulatus* RCs where the Q_B site was mutated to contain 42 residues from the Q_A site. The RCs have M220–M261 in the Q_A site substituted for L193–L227 in the Q_B site plus the M subunit second-site mutations, M144MI and M145AS, which had been found to restore the ability of the bacteria to grow photosynthetically. These mutants lack L210D, L212E, L213D, and L223S which have been previously shown to affect the electron transfer from Q_A^- to Q_B. Despite the large change in the Q_B pocket, secondary quinone function still can be reconstituted. The UQ_4 dissociation constant for the Q_B site in the mutant is only three times as large as in the wild type RCs. The rate of charge recombination ($P^+Q_AQ_B^- \rightarrow PQ_AQ_B$) ($k_{BP}$) is reduced from 8.9 s^{-1} in wild type RCs to 0.05s^{-1} in the mutant, This indicates that $Q_AQ_B^-$ is stabilized relative to $Q_A^-Q_B$ by at least 60 meV more than in wild type protein. k_{BP} is pH independent in the mutant RCs, while in wild type RCs k_{BP} increases at alkaline pHs as reduction of Q_B becomes energetically less favorable. Similar pH independent, slow k_{BP} has been found in the L212EA/L213DA double mutant. The largest change found in the mutant is that the electron transfer from Q_A^- to Q_B ($k_{AB}^{(1)} \approx 14\ s^{-1}$) is 3 orders of magnitude slower than in wild type RCs ($10^4\ s^{-1}$).

Introduction

The primary process of bacterial photosynthesis occurs within reaction centers (RCs), a membrane-bound pigment–protein complex. RCs convert light energy into chemical free energy via a series of transmembrane electron transfer reactions between protein associated redox cofactors. X-ray crystal structures of RCs from the purple non-sulfur bacteria *Rhodopseudomonas viridis* and *Rhodobacter sphaeroides* show a surprising c_2 symmetry of the redox cofactors (Komiya et al. 1988; Deisenhofer and Michel 1991; Lancaster et al. 1995) (Figure 1). A dimer of bacteriochlorophylls (P) lies near the center of the symmetry axis near the periplasm. Moving along the transmembrane direction are 2 bacteriochlorophyll monomers (B_L and B_M), 2 bacteriopheophytins (H_L and H_M) and 2 ubiquinone-10 (UQ_{10}) molecules (Q_A and Q_B). However, the symmetry related cofactors behave quite differently. Electron transfer proceeds from an excited singlet state of P, which reduces H_L in 3 ps via B_L. H_L^- then transfers an electron to Q_A in 200 ps. Q_A^- then reduces Q_B. B_M and H_M are inactive. Q_A, is a non-exchangeable redox cofactor which never binds protons. Little proton uptake by the protein is coupled to Q_A reduction. In contrast, quinone from the membrane quinone pool freely exchanges into the Q_B binding site and forms a doubly reduced product. Amino acids near Q_B bind protons to stabilize the anionic semiquinone formed after the first stage of reduction (Takahashi and Wraight 1994; Okamura and Feher 1995). Two protons are transferred to the reduced quinone at the

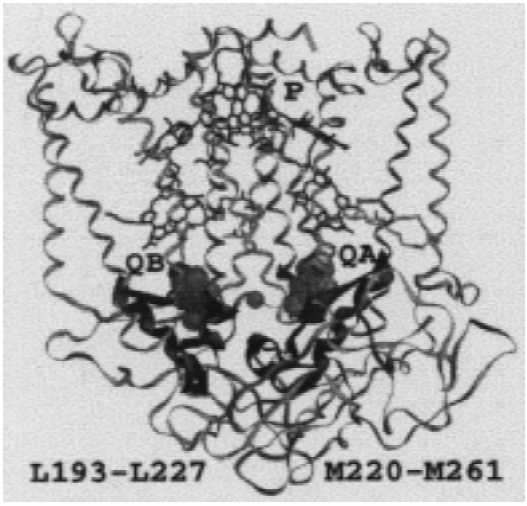

Figure 1. The A6D1 mutant was generated by replacing His^{L190}-Gly^{L228} in the Q_B site with His^{M217}-Gly^{M262} from the analogous region of the Q_A site (Table 1). The two mutations M144Met to Iie and M145Asn to Ser in the photosynthetically competent A6D1 lie between Q_B and H_M. The *Rb. sphaeroides* RC structure is shown (Stowell et al. 1997). These RCs have 78.3, 76.5 and 64.5% sequence identity with the L, M and H chains of *Rb. capsulatus* RCs studied here (Williams et al. 1986). In the duplicated region of the M subunit, there are only 3 conservative changes while there are 5 changes in the L subunit that is removed.

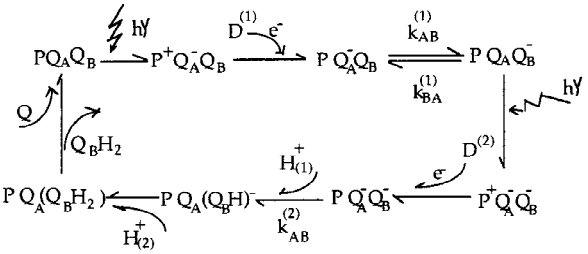

Figure 2. The photochemical cycle in RCs. *The first photon*. When ground state RCs absorb light, P is excited and a electron is transferred by way of H_L to the first primary quinone Q_A forming $P^+Q_A{}^-Q_B$ (if there is no Q_B and no electron donor this returns to the ground state at k_{AP}). One electron donor such as cytochrome c/RC will reduce P^+ in microseconds ($D^{(1)}$). $Q_A{}^-$ reduces the secondary quinone bound at the Q_B site to form $P^+Q_AQ_B{}^-$ (at $k_{AB}{}^{(1)}$). $Q_A{}^-$ to Q_B electron transfer and reduction of P^+ occur independently. *The second photon.* If Q_A has been oxidized by Q_B, formation of a second P^+ will cause Q_A to be reduced again. A second electron donor/RC can reduce P^+ ($D^{(2)}$). This can then transfer an electron to $Q_B{}^-$ (at $k_{AB}{}^{(2)}$). The first proton is bound by $Q_B{}^-$ and the second by the doubly reduced Q_BH^-. Q_BH_2 leaves the RCs, a quinone binds to the Q_B side and the cycle can start again.

appropriate stages in the reaction cycle to produce dihydroquinone which is released into the membrane and replaced with the substrate quinone (Figure 2).

RCs from *Rb. sphaeroides* and the closely related *Rb. capsulatus* have three protein subunits, L, M and H. The crystal structures of *Rb. sphaeroides* RCs show that L and M each have 5 transmembrane helices (Komiya et al. 1988; Deisenhofer and Michel 1991; Lancaster et al. 1995). All of the cofactors are bound by these subunits. H, with only one transmembrane helix, caps the cytoplasmic side of the protein near the quinones. L and M are arranged with approximate c_2 symmetry around the redox cofactors. The transmembrane helices of the L polypeptide surround B_L and H_L while B_M and H_M are associated with the M chain The chains cross near the cytoplasm so that the M subunit binds Q_A and L binds Q_B. The sequence identity between the L and M chains is 31.9% in *Rb. capsulatus* and 33.9% in *Rb. sphaeroides* RCs (Williams et al. 1986). With this degree of sequence identity, it is likely that RCs were originally made of identical subunits that evolved into the modern protein.

The quinone binding sites are made up of regions where there is less homology between L and M subunits. *Rb. capsulatus* RCs were genetically engineered to explore the behavior of a more symmetric protein (Coleman and Youvan 1993). Two regions with similar positions in the structure, but with low sequence identity were selected. Forty-two residues, M220 to M261, from the Q_A binding site replace the 35 residues, L193 to L227, in the Q_B binding site (Figure 1, Table 1). BLAST finds no significant similarity between the 2 segments. Eight residues, clustered near the ends of the sequences, are the same (Table 1). Each sequence contains the last residues of the 4th and 5th transmembrane helix, as well as a smaller connecting helix that runs parallel to the protein surface. Q_A and Q_B sit within the region bounded by the 3 helices. Thus, in the mutant many of the residues near Q_B are replaced by residues from the Q_A site. Of the 18 residues within 4 Å of Q_B in the *Rb. sphaeroides* RC structure 1AIG (Stowell et al. 1997), 11 are in the segment of the L subunit that are replaced. Earlier studies have found many of the residues removed from the Q_B site are important for function. In particular mutations of Asp L210, L213, Glu L212 and Ser L223 have been characterized in *Rb. sphaeroides* and *Rb. capsulatus* RCs (see (Takahashi and Wraight 1994; Okamura and Feher 1995) for reviews).

Bacteria with the segment substitution were found to be unable to grow photosynthetically. A photosynthetically competent strain, A6D1, was identified with an intact Q_A insert. MetM144 was found to be changed to Ile and AlaM145 to Ser. These residues lie between Q_B and H_M. Thus, RCs with the segment substitution can carry out the complete photocycle

Table 1. BLAST alignment of relevant portion of *Rb. capsulatus* L and M subunits

```
                123456789 123456789 123456789 123456789 12
210   GSALLFAMHGATILAVTRFGGERELEQIVDRGTASERAALFWRWTMGFNATMEGIHRWAI 269 M
Hel   TTTTTTTTTTTTTTT        PPPPPP   PPPPPPPPPPPPPP        TTTTTT
Ali    +A   AMHGA +L+     + +            +    ++R  MG++    GIHR  +
183   TTAWALAMHGALVLSAANPVKGKTMR-------TPDHEDTYFRDLMGYSVGTLGIHRLGL 235 L
Hel   TTTTTTTTTTTTTTTTT                PPPPPPPPPPPP    TTTTTTTTTT
      3456789 123456789 12345678       9 123456789 12345678
```

The region removed from the L subunit and the replaced region of the M subunit are underlined. Without counting the identical residues on the ends of the segments 42 residues from M replace 35 residues plus a 7 residue gap in the L subunit. Ali:+ are similar residues; HEL: marks the helical regions: T is transmembrane helix, P a helix parallel to the membrane. The program DSSP (Kabsch and Sander 1983) was used to determine the helical segments in the homologous *Rb. sphaeroides* RC structure 1AIG (Stowell et al. 1997).

(Figure 2) at a rate that can support growth. The work reported here characterizes the steps in the reaction sequence that involve quinone in isolated A6D1 RCs. The changes in the affinity of quinone for the protein and in the kinetics and thermodynamics of the various quinone involved reactions were determined and compared with wild type protein.

Materials and methods

The genetic modification of the RCs used to obtain the *Rb. capsulatus* A6D1 mutant has been described previously (Coleman and Youvan 1990, 1993). Wild type and mutant bacteria were grown in the dark. RCs were isolated by the protocol of Prince and Youvan (1987) with some modification. Lauryldimethylamine N-oxide (LDAO) was used to solubilize the chromatophore membranes. The protein was isolated by ion-exchange chromatography on a DEAE Biogel-A column. The A6D1 RCs were eluted from the column with 150 mM KCl, 0.05% LDAO, and 10mM potassium phosphate at pH 7.3. The RC concentration was determined at 802 nm or 865 nm using the extinction coefficients: ϵ_{802}=0.288 μM^{-1} cm^{-1} or ϵ_{865}=0.135 μM^{-1} cm^{-1}, respectively. Kinetic measurements were carried out with 0.5–1.0 μM RCs.

The presence of H, M and L subunits in the mutant RCs was determined by a protein chip assay. Three polypeptides with appropriate molecular weight were found using the SELDI-TOF/MS system from Ciphergen Biosystems, Inc. (Palo Alto, CA. SELDI: Surface Enhanced Laser Desorption Ionization) (Hutchens and T.-T.Yip 1993).

UQ_4 (Sigma) was solubilized in alcohol. Caps, Ches, Tris, phosphate and Mes were used as pH buffers at the appropriate pH. Horse heart cytochrome *c* (Sigma) was reduced with sodium borohydride (Sigma). The pH indicator dyes were chlorophenol red and cresol red (Sigma). The semiquinone was trapped using 100 μM ferrocene (Aldrich) as an electron donor to reduce $P^{+\cdot}$.

Time-resolved optical spectroscopy was performed with a flash spectrometer from the University of Pennsylvania Biomedical Instrumentation Group. A 10 μs xenon flash initiated the reaction. Measurements were carried out at single wavelengths using a continuous illumination light source. A shutter was closed between measurements. Data was collected by a Thorn photomultiplier with the data stored on a LeCroy 300 MHz oscilloscope. Kinetic transients were fit assuming exponential decays using IGOR Pro (WaveMetrics). Two 10 μs Xenon flashes spaced at the appropriate intervals was used for the cytochrome *c* double flash experiment.

For measurements of cytochrome *c* oxidation under conditions of steady state turnover, RCs were illuminated from a direction perpendicular to the measuring beam. A 100 W Oriel tungsten halogen lamp provided the source of the continuous illumination. The intensity was 300 mw cm^{-2}. A >700 nm long pass filter was used. The change in absorption when one equivalent of cytochrome *c* is oxidized per RC was determined from the absorption change at 550 nm after a single, saturating flash.

The kinetics of the electron transfer that returns $P^+Q_A^-$ or $P^+Q_AQ_B^-$ to the ground state (k_{AP}^{obs} and k_{BP}^{obs}, respectively) were measured at 425 nm, a maximum of the absorption difference between P^+ and P. The semiquinone signals of Q_A^- and Q_B^- were monitored at 450 nm a maximum in the difference in

Q^- and Q absorption. Cytochrome *c* oxidation was monitored at 550 nm where the absorbance difference between cyt c^{2+} and cyt c^{3+} has a maximum.

Flash-induced proton uptake was measured optically using the pH-indicator dyes chlorophenol red and cresol red (Takahashi and Wraight 1992; Paddock et al. 1994) at the isosbestic for the difference between PQ_A and $P^+Q_A^-$ near 575 nm. The unbuffered assay solution contained 50 mM KCl, 40 μM pH indicator dye, 100 μM Q_4, 0.03% Triton x-100, 100 μM ferrocene and 1 μM RC. Samples were degassed under nitrogen. Control measurements were made with 10 mM buffers. The net proton uptake was derived by subtracting the signals of the buffered controls from the unbuffered samples. HCl was used to determine the change in dye absorption per proton.

Use of the charge recombination in the $P^+Q_B^-$ state to determine the free energy difference between $P^+Q_A^-$ and $P^+Q_B^-$

Charge recombination occurs by 2 paths. The observed rate (k_{BP}^{obs}) is:

$$k_{BP}{}^{obs} = k_{BP} + k_{BAP} = k_{BP} + k_{AP}/(K_{AB} + 1) \quad (1)$$

where k_{BP} is the rate of direct electron tunneling from Q_B^- to P^+ (Takahashi and Wraight 1992; Labahn et al. 1994; Labahn et al. 1995; Allen et al. 1998) and k_{BAP} is the rate of an indirect path involving charge recombination from $P^+Q_B^-$ via $P^+Q_A^-$ which then returns to the ground state by electron tunneling from Q_A^- to P^+. On the indirect path $P^+Q_B^-$ and $P^+Q_A^-$ remain at equilibrium. K_{AB} is $[Q_AQ_B^-/Q_A^-Q_B]$ and $(K_{AB}+1)^{-1}$ is the fraction of the total reduced quinone ($Q_A^- + Q_B^-$) where the electron is on Q_A. The difference in free energy between the $Q_A^-Q_B$ and $Q_AQ_B^-$ states, can be determined from $-\Delta G_{AB}=RT \ln K_{AB} = RT \ln (k_{AP}/k_{BAP} - 1)$ (Kleinfeld et al. 1984; Mancino et al. 1984). In wild type RCs, K_{AB} can be increased by reconstituting Q_A with low potential quinones, resulting in very slow charge recombination by direct electron transfer from Q_B^- to P^+. When charge recombination is primarily by the direct route, which is relatively insensitive to the energy of the $P^+Q_B^-$ state, k_{BP}^{obs} is slower than $\approx 0.2\ s^{-1}$ (Allen et al. 1998).

Distribution of reaction centers after successive flashes in the cytochrome c *double flash experiment*

In the presence of an exogenous electron donor such as reduced cytochrome *c*, P^+ is reduced and the electron is trapped on Q_A or Q_B following the first flash (Figure 3). All RCs oxidize a cytochrome electron donor ($D^{(1)}$). On the next flash no stable P^+ is produced if RCs are in the state PQ_A^- and no additional cytochrome will be oxidized ($D^{(2)}$=0). If RCs were in the $PQ_AQ_B^-$ state, a second flash can transfer an electron to Q_A leaving new P^+ to be reduced by a second cytochrome *c* ($D^{(2)}$). Thus, the ratio of $D^{(2)}/D^{(1)}$ provides the fraction of the RCs where the electron has moved from Q_A^- to Q_B at the time of the second flash (Parson 1969).

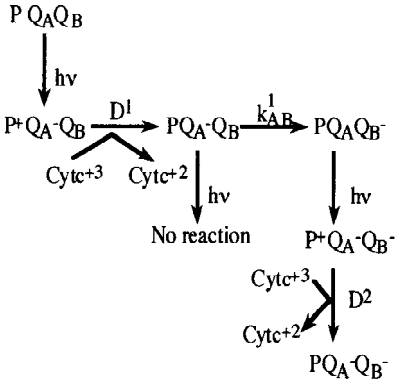

Figure 3. The cytochrome *c* double flash method. If the electron on Q_A^- has not moved to Q_B then no cytochrome *c* is oxidized after the second flash. $D^{(2)}/D^{(1)}$ is equal to $[Q_AQ_B^-]/([Q_A^-Q_B]+[Q_AQ_B^-])$ where the denominator is the total RC population.

Determination of the affinity of the quinone for the Q_B site

The dissociation constant for the quinone from the Q_B site (K_d) was determined by titration with UQ_4. As in a standard analysis, $K_d = [RC_F][Q_F]/[RC{\bullet}Q_B]$ where RC_F is the concentration of RCs without Q_B and Q_F is the free UQ_4 in solution. $RC{\bullet}Q_B$ are RCs with UQ_4 bound to the Q_B site. The total UQ_4 ($[Q_T]$) added is $[Q_F]+[RC{\bullet}Q_B]$ and the total RCs ($[RC_T]$) is $[RC_F]+[RC{\bullet}Q_B]$. The dissociation constants (K_d) of the UQ_4 at the Q_B site was calculated using PeakFit (Jandel Scientific) to obtain a non-linear least squares fit to the relationship:

$$\%Q_B = \frac{[RC \bullet Q_B]}{[RC_T]} = \frac{1}{2}\left\{\left(1 + \frac{[Q_T] + K_d}{[RC_T]}\right) - \sqrt{\left(1 + \frac{[Q_T] + K_d}{[RC_T]}\right)^2 - 4\frac{[Q_T]}{[RC_T]}}\right\} \quad (2)$$

[RC•Q_B] was obtained either from the amplitude of the slow phase of charge recombination in the absence of donor to P^+ or from the cytochrome c double flash experiment.

Results and analysis

Charge separation to form $P^+Q_A^-$ and charge recombination from this state in A6D1 RCs

With no extra ubiquinone added, the amount of $P^+Q_A^-$ per RC formed after a flash was the same in wild-type and mutant protein. Thus, Q_A remains bound to the mutant RCs during protein isolation. Approximately 98% of wild-type RCs that absorb a photon produce $P^+Q_A^-$ (Wraight and Clayton 1973). The amplitude of the $P^+Q_A^-$ formed on a flash in the mutant shows that the relative quantum yield is comparable in mutant and wild type RCs. The high quantum yield shows that H_L^- in the first intermediate state ($P^+H_L^-$) is able to reduce Q_A faster than the $P^+H_L^-$ returns to the ground state (Gunner and Dutton, 1989).

Charge recombination in $P^+Q_A^-$ RCs occurs by direct electron transfer from Q_A^- to P^+. The $P^+Q_A^- \rightarrow PQ_A$ reaction occurs as anearly single exponential process with a rate (k_{AP}^{obs}) of 8 s^{-1} in both wild type and mutant RC (data not shown). Thus, the large scale modification of the Q_B site has little or no impact on the Q_A reduction or oxidation reactions that involve H_L or P.

Charge recombination from the $P^+Q_B^-$ state as a measure of ΔG_{AB} in the mutant

In the presence of excess UQ_4 the rate of the reaction $P^+Q_B^- \rightarrow PQ_B$ (k_{BP}^{obs}) is 0.02 s^{-1} (Figure 4A). This is significantly slower than in the wild type RCs where k_{BP}^{obs} is 0.85 s^{-1} and k_{AP} is 8 s^{-1}, K_{AB} is 8.4 and ΔG_{AB} is 55 meV. In the A6D1 mutant, the back reaction from $P^+Q_B^-$ is sufficiently slow that it appears to occur by direct charge recombination (k_{BP}) rather than by the uphill reaction of reform $Q_A^-Q_B$ (k_{BAP}). The decrease in k_{BP}^{obs} shows that $Q_AQ_B^-$ is stabilized relative to $Q_A^-Q_B$ by at least 60 meV in the mutant (see equation 1). This could occur by raising the energy level of $Q_A^-Q_B$ or by lowering that of $Q_AQ_B^-$. However, when the $Q_A^-Q_B$ state energy is raised, k_{AP}^{obs} becomes faster as a second route for charge recombination via an uphill reaction that reforms $H_L^-Q_A$ becomes important (Gunner et al. 1982; Woodbury et al. 1986). This does not happen in the mutant as k_{AP}^{obs} is the same as in the wild type RCs. Thus, the change of the Q_B site stabilizes the Q_B^- semiquinone by at least 60 meV relative to the wild type RCs so that ΔG_{AB} is at least −120 meV.

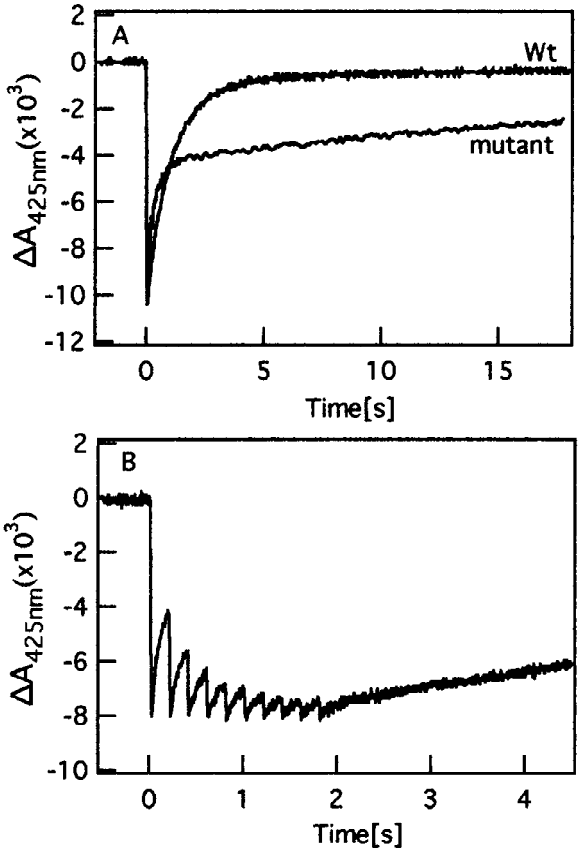

Figure 4. Charge separation and recombination monitored by the absorbance change at 425 nm as a function of time. 0.5 μM RCs, 100 μM UQ_4, 0.04% LDAO, pH 7.3. The rate constants are (A) Wild type RCs k_{AP}= 7.6 s^{-1}, k_{BP}= 0.85 s^{-1}; mutant, k_{AP}= 7.4 s^{-1}, k_{BP}= 0.027 s^{-1}. Approximately, 50% of the reaction occurs at k_{AP} in the mutant. (B) Mutant RCs repetitively excited at an interval of 0.2 s.

The pH dependence of the charge recombination reaction in $P^+Q_B^-$ RCs

The pH dependence of the rate at which $P^+Q_AQ_B^-$ returns to the ground state (k_{BP}^{obs}) was determined for wild type and mutant RCs (Figure 6). As seen previously, in wild type RCs k_{BP}^{obs} increases with pH below pH 6 and above pH 9 and is pH independent in between (Maroti et al. 1994). In contrast, the charge recombination rate k_{BP} for A6D1 RCs is essen-

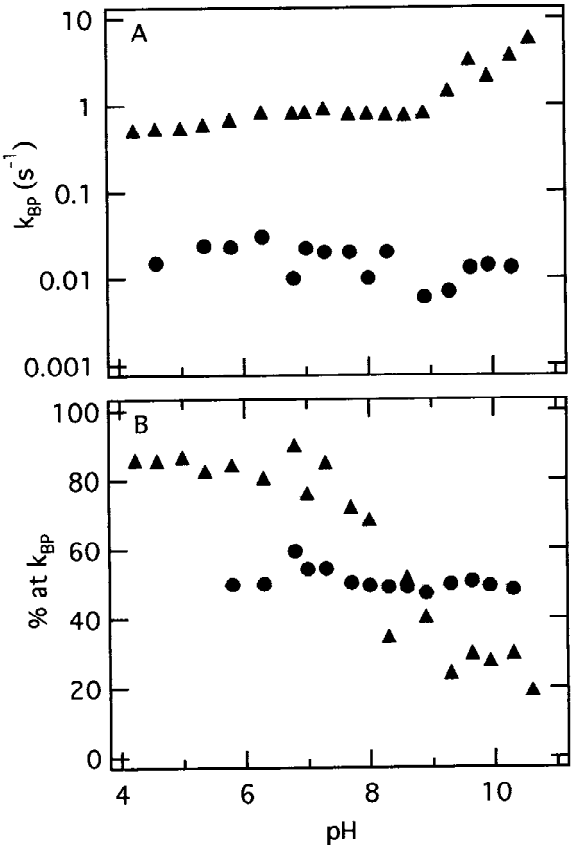

Figure 5. (A) pH dependence of the $P^+Q_AQ_B^-$ decay rate (k_{BP}^{obs}). (B) Fraction of the charge recombination at the slow rate indicative of RCs in the $P^+Q_AQ_B^-$ state. In wild type RCs, at pH less than 7, k_{BP}^{obs} accounts for 90% at pH 7 but it decreases to 30% at pH 9 and above. However, for the mutant RCs, the amplitude at k_{BP} was constant at ≈50%. 0.3 μM RCs, 100 μM UQ_4, 10 mM buffer. • AD61; ▲ wild type RCs.

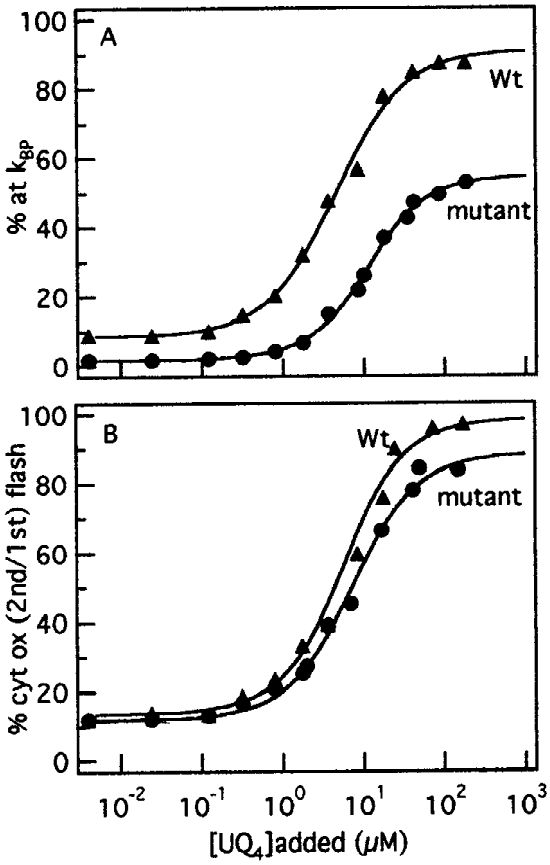

Figure 6. UQ_4 titration of the Q_B site of RCs from wild type and A6D1 RCs. Percentage of RCs with behavior characteristic of having an active Q_B. (A). The charge recombination assay for Q_B binding. % at k_{AB} is = ΔA(decaying at k_{BP})/ΔA(total) after first flash. ΔA measured at 425 nm. K_d is 4.4 ± 0.5μM for wild type and 11.9 ± 0.6μM for mutant RCs. (B). The cytochrome *c* double flash assay for Q_B reduction prior to the second flash (see Figure 2). All RCs oxidize a cytochrome on first flash. Electron transfer from Q_A^- to Q_B is required for cytochrome oxidation following the second flash. Cytochrome oxidation measured at 550 nm with 20 μM horse heart cytochrome *c* added. Flashes are spaced 0.5 s apart. K_d's are 7.8 ± 0.9 μM and 11 ± 0.6 μM, respectively, for wild type and mutant RCs. 0.5 μM RCs, 100 μM UQ_4, 0.04% LDAO, pH = 7.3.

tially pH independent from pH 4.6 to 10.3, with k_{BP}^{obs} ≈0.02 s^{-1}.

In wild type RCs at pH 7–8, 90% of the RCs will form $P^+Q_B^-$ after a single flash. At high pH, the amplitude of the slow, $P^+Q_B^-$, phase decreases to as little as 30% (Figure 5B). In contrast as will be described below only 50% of the A6D1 RCs form $P^+Q_B^-$ following a single flash. However, this amplitude is independent of pH (Figure 5A).

The affinity of ubiquinone for the Q_B site

The affinity of UQ_4 for the Q_B site was determined for the wild type and A6D1 RCs. The fraction of UQ_4 bound can be measured in two different ways. The distribution of $P^+Q_A^-$ and $P^+Q_B^-$ RCs is easy to determine from the charge recombination kinetics (Figure 6). With no electron donor to reduce P^+, the rate of return to the ground state in $P^+Q_A^-$ is 8 s^{-1} in both mutant and wild type RCs. It is 0.02–0.05 s^{-1} from $P^+Q_B^-$ in A6D1 and 0.85 in wild type RCs (Figure 4). Although the term K_d will be used here, the population of $P^+Q_B^-$ can overestimate Q_B affinity (Wraight and Stein 1980, 1983). Quinone can bind to the Q_B during the lifetime of $P^+Q_A^-$, while reduced Q_B^- has a much reduced dissociation rate. The increase in the fraction of charge recombination at the slow rate with increasing UQ_4 provides a K_d

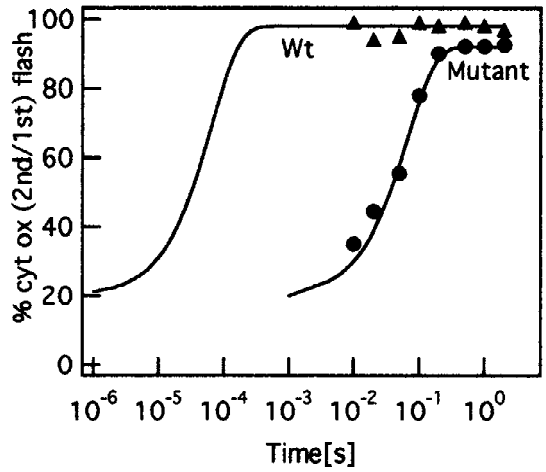

Figure 7. Electron transfer from Q_A^- to Q_B measured with the cytochrome *c* double flash method (see Figure 3). The cytochrome $\Delta A(\text{2nd flash})/\Delta A(\text{first flash}) = D^{(2)}/D^{(1)}$ (Figure 2) was monitored at 550 nm as a function of the spacing between first and second flash at pH 7.3. The electron transfer rate ($k_{AB}{}^{(1)}$) for the mutant of 14 s^{-1} is obtained from $\Delta A_1/\Delta A_2 = 1-\exp(-(k_{AB}{}^{(1)}*\Delta t))$ (Parson 1969). The curve for the wild type RCs was simulated using values of $k_{AB}{}^{(1)}$ = 15,400 s^{-1} (τ = 65 μs) from Baciou et al. (1993) is provided for comparison.

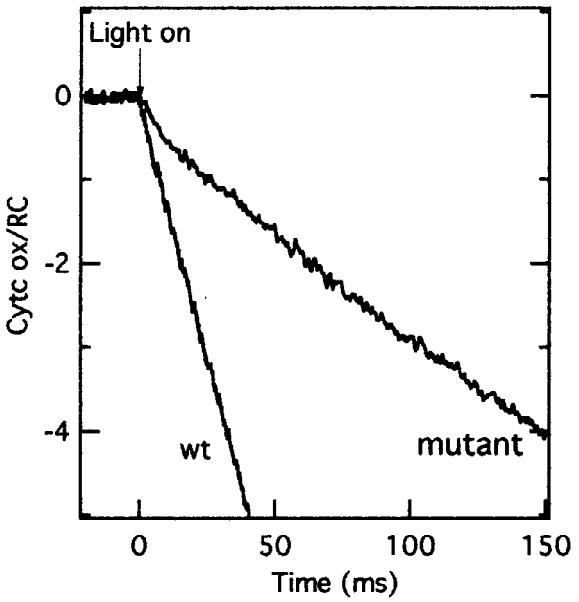

Figure 8. Steady state cytochrome *c* oxidation with wild type and mutant RCs monitored by the absorbance change at 550 nm under continuous illumination. 0.6 μM RC, 20 μM cyt *c*, 100 μM UQ_4, 0.04% LDAO, at 24 °C, I ≈600 mW. The vertical scale was normalized given ΔA for 1 cyt c/RC obtained from the absorbance change at 550 nm after a single saturating flash.

value for the wild type of 4.4 ± 0.5 μM and 11.9 ± 0.6 μM for the mutant. Thus, despite the large scale rearrangement of the Q_B site, the affinity of the binding site for UQ_4 is weakened by less than a factor of three. However, when the RCs are saturated with UQ_4 charge recombination is at the slow rate characteristic of $P^+Q_B^-$ in 90% of the wild type but only 50% of the mutant RCs. Thus, the yield of $P^+Q_B^-$ is significantly smaller in the mutant RCs than in the wild type protein.

A second measure of the Q_B site occupancy is the ratio of cytochrome *c* oxidation on the first ($D^{(1)}$) and second ($D^{(2)}$) flash (Figure 3). With flashes spaced 0.5 s apart, the K_d of UQ_4 for the Q_B site is 7.8 ± 0.9 μM and 11 ± 0.6 μM. The fraction of RCs that can form $P^+Q_B^-$ at saturating UQ_4 is 98% and 90%, respectively, for wild type and mutant RCs (Figure 6B). There is good agreement between the K_d's determined by the cytochrome double flash method and the measurement of the rate of return to the ground state when no electron donor is present. However, with the cytochrome *c* assay, almost all RCs form $P^+Q_B^-$.

Why only half the RCs form $P^+Q_B^-$ in A6D1 RCs when there is no electron donor to reduce P^+

When the Q_B site is saturated with UQ_4 only 50% of the charge recombination occurs at a rate characteristic of $P^+Q_B^-$ RCs (k_{BP}) while 50% is at the faster k_{AP}. However, with repetitive excitation, on each additional flash half the population that returned to the ground state at k_{AP} now shows the slower recombination rate characteristic of RCs in the state $P^+Q_B^-$ (Figure 3B). After a series of flashes, all RCs return to the ground state at the slow rate. Thus, it is not that half the RCs have an incompetent Q_B site. Rather it appears that the quantum yield for formation of $P^+Q_B^-$ is only 50%. Thus, the state $P^+Q_A^-$ can either produce $P^+Q_B^-$ (at $k_{AB}{}^{(1)}$) or the ground state (at k_{AP}). The quantum yield is $k_{AB}{}^{(1)}/(k_{AB}{}^{(1)}+k_{AP})$. If these 2 rates are equal only half the RCs reach $P^+Q_B^-$ after each flash. By repeating the partitioning between ground and $P^+Q_B^-$ states following a series of flashes all the RCs form the long-lived $P^+Q_B^-$. This suggests that $k_{AB}{}^{(1)}$ is ≈8 s^{-1}. Following the first flash, the fraction of charge recombination that occurs at the fast rate (k_{AP}) remains at ≈50% from pH 5.5 to 10.5 (Figure 5). Thus $k_{AB}{}^{(1)}$ appears to be relatively independent of pH.

The observation that 90% of the RCs reach the $P^+Q_B^-$ state with cytochrome *c* added (Figure 6B) is further evidence that competition with charge recombination from the $P^+Q_A^-$ state limits the formation of $P^+Q_B^-$. With the addition of cytochrome c the back

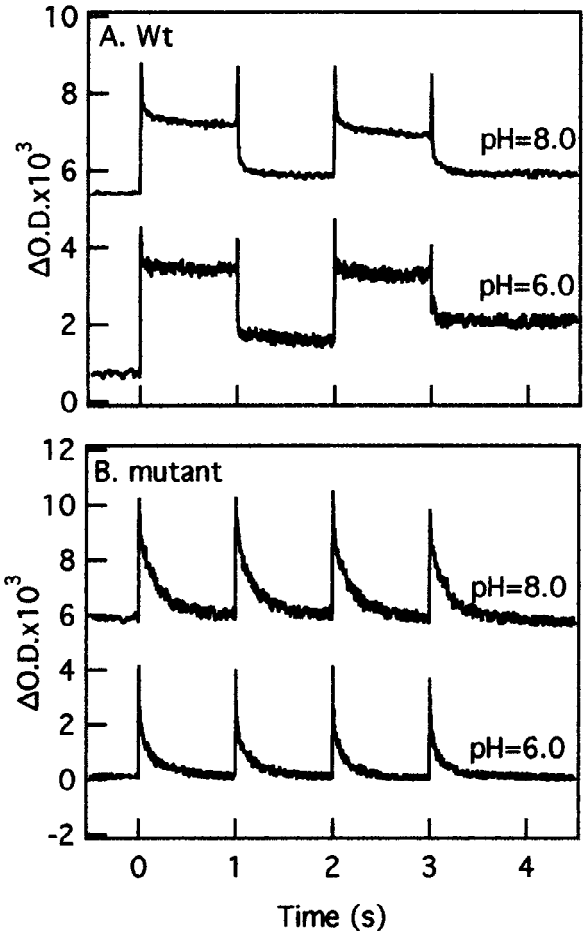

Figure 9. Semiquinone anion formed after a series of saturating flashes spaced 1 s apart monitored at 450 nm. 0.5 μM RCs, 100 μm UQ_4, and 100 μM ferrocene, 10 mM buffer, 0.04% LDAO. at pH 6 and pH 8. (A) Wild type RCs. The first flash shows formation of $(Q_A^- + Q_B^-)$ with the electron primarily on Q_B. This is stable for seconds. The semiquinone disappears after the second flash as QH_2 is formed. (B) AD61 RCs. In the mutant, the semiquinone decays at $\approx 7\ s^{-1}$ after each flash.

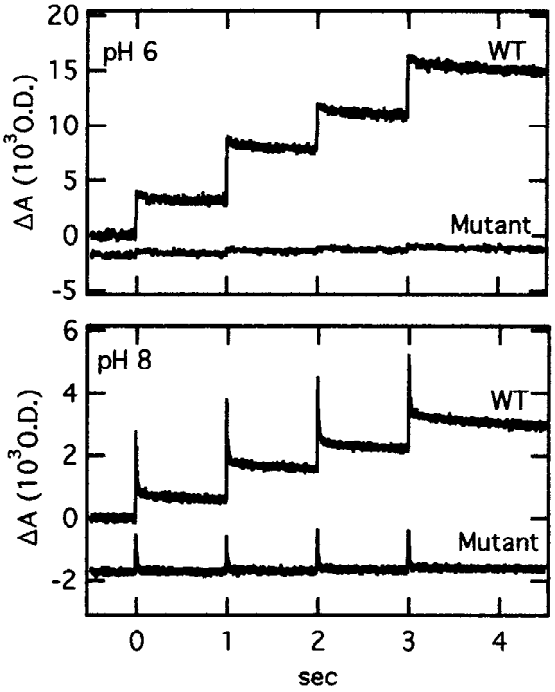

Figure 10. Proton uptake for wild type and A6D1 RCs. 1 μM RCs, 0.03% Triton, UQ_4=150 μm, 100 μM Ferrocene, 50 mM KCL. At pH 6, 50 μM chlorophenol red monitored at 575 nm. At pH 8, 50 μM cresol red measured at 555 nm.

reaction is blocked by the fast rereduction of P^+ by the cytochrome. Here all electron transfer can go forward to form $P^+Q_B^-$.

There is a second measure of the rate of electron transfer from Q_A^- to Q_B which relies on the cytochrome *c* double flash method (Figure 7). Since cytochrome *c* oxidation on the second flash is not seen if Q_A is still reduced, the ratio of cytochrome *c* oxidized on the first ($D^{(1)}$) and second flash ($D^{(2)}$) can be used to assay the electron transfer rate from Q_A to Q_B (Figure 3). As the interval between flashes increases providing more time for more electron transfer from Q_A^- to Q_B, more cytochrome *c* is oxidized on the second flash. The fraction of RCs where the electron has already been transferred to Q_B is $(D^{(2)})/(D^{(1)}) = 1 - \exp(-(k_{AB}{}^{(1)} * \Delta t))$ (Parson 1969). Varying the time interval, Δt, between the first and second flashes, the observed rate of electron transfer from Q_A^- to Q_B was determined to be 14 s^{-1}. This value is comparable to that estimated from the $\approx$50% quantum yield for formation of $P^+Q_B^-$. At a given time interval between flashes, the amplitude of the cytochrome *c* oxidized on the 3rd and 4th flash is comparable to the that found on the 2nd flash. The third oxidation of P relies on the electron transfer from Q_A^- to Q_B^- ($k_{AB}{}^{(2)}$). If $k_{AB}{}^2$ were slower than $k_{AB}{}^{(1)}$, $D^{(3)}$ would be smaller than $D^{(2)}$ (Figure 2).

Steady state turn over in A6D1 RCs

The overall rate of the photocycle was determined from the oxidation of cytochrome c at 550 nm in the presence of excess UQ_4 (Figures 2 and 8) (Paddock et al. 1989, 1990). Slowing either the electron or proton transfer at any step will result in a decrease of the turnover rate. In wild type RCs, the steady state cytochrome *c* turnover rate is 120 (cyt *c*/RC) s^{-1},

consistent with previous results (Bylina and Youvan 1987). The mutant shows a fast oxidation of about 0.8 cyt/RC followed by a slower steady-state rate of 24 (cyt *c*/RC) s^{-1}. This suggests that the formation of the state $P^+Q_A^-$ oxidizing one cytochrome *c* per RC is unimpaired. However, the second cytochrome *c* oxidation which requires electron transfer from Q_A^- to Q_B is slow. As the rate is constant following the second cytochrome oxidation/RC the electron transfer from Q_A^- to Q_B appears to be the rate limiting step for the entire photocycle.

Semiquinone stability and proton binding

The stability of the semiquinone in the RCs can be determined at 450 nm in RCs with an electron donor to reduce P^+ and block the return to the ground state. In wild type RCs, the first flash forms the semiquinone $Q_AQ_B^-$. This state is stable for seconds (Figure 9A). The second flash forms the dihydroquinone Q_BH_2 as seen from the disappearance of the semiquinone signal (Wraight 1977; Baciou et al. 1993). Binding UQ_4 to the Q_B site allows the cycle to start again (Figure 1). In the A6D1 RCs, when the electron donor ferrocene but no UQ_4 is added, the semiquinone at Q_A is stable for many seconds. However, when Q_B is reconstituted, no stable Q_B^- was observed (Figure 9B). Rather absorption at 450 nm decays to the baseline at a rate of $\approx 7\ s^{-1}$ after each flash.

Protons are bound by RCs and transferred to Q_B during the electron transfer cycle (Figure 2). Proton binding was monitored from the absorbance changes of pH indicator dyes (Figure 10). In wild type RCs protons are taken up on each flash. As expected, fewer protons were bound on the first flash where proton uptake is by the protein than the second flash which forms QH_2 (Maroti and Wraight 1988; Takahashi and Wraight 1992; McPherson et al. 1993). In contrast, very little proton uptake by the A6D1 RCs after any flash at either pH 6 or 8.

Discussion

The properties of Q_A and Q_B have been investigated in a revertant of the segment substitution mutant of *Rb. capsulatus* RC where the 42 residues, M220–M261, from the Q_A binding site replace the 35 residues, L193–L227, in the Q_B binding site (Coleman and Youvan 1993). Despite this large change, these bacteria grow photosynthetically in the A6D1 revertant which has added two additional mutations between the Q_B site and the nearby bacteriopheophytin. Thus, at least in whole cells, a complete photocycle leading to the production of QH_2 occurs rapidly enough to support growth. Detailed characterization of the isolated mutant protein identifies how RC function is affected by the changes in Q_B site structure.

The Q_B site, which is modified substantially, still binds ubiquinone (UQ_4) with an affinity that is only three times weaker than in wild-type protein. The most dramatic change in the reaction is the slowing of the first electron transfer from Q_A^- to Q_B (k_{AB}^1) from $\approx 5000\ s^{-1}$ in wild type RCs (Okamura and Feher 1995) to $\approx 10\ s^{-1}$ in the A6D1 RCs.

The large scale sequence substitution in the A6D1 mutant has little impact on the tunneling reactions from either Q_A^- or Q_B^- to P^+. The rate of the reaction $P^+Q_A^- \rightarrow PQ_A$, which occurs by direct electron tunneling from Q_A^- to P^+, is unchanged from that found in wild type RCs. The rate of the reaction $P^+Q_B^- \rightarrow PQ_B$ (k_{BP}^{obs}) is much slower than in wild type RCs. This behavior has been shown in simpler, single site Q_B mutants to indicate that the mutation stabilizes $Q_AQ_B^-$ relative to $Q_A^-Q_B$ by at least 60 meV relative to the wild type protein (Takahashi and Wraight 1990; Paddock et al. 1997). This is, as expected, due to a change in the Q_B^-/Q_B midpoint rather than the Q_A^-/Q_A midpoint.

As $-\Delta G^\circ_{AB}$ increases, charge recombination from $P^+Q_B^-$ occurs by the free energy insensitive direct electron tunneling from Q_B^- to P^+. The direct tunneling rate from Q_B^- to P^+ is similar to that that found in more limited Q_B site mutants that change AspL213 (Takahashi and Wraight 1990, 1992; Hanson et al. 1992; Maroti et al. 1994; Paddock et al. 1994). In the L213 single mutants k_{BP}^{obs} is slow but increases with increasing pH (Paddock et al. 1990). The segment substitution in the A6D1 RCs replaces both L212 and L213 with Ala (Table 1). Double mutants of *Rb. capsulatus* or *Rb. sphaeroides* RCs that replace GluL212 and AspL213 with non-ionizable residues show a slow k_{BP}^{obs} with no pH dependence, similar to the A6D1 RC (Takahashi and Wraight 1992; Baciou et al. 1993).

Evidence for a bound Q_B^- in A6D1 RCs

The very slow back reaction (k_{BP}^{obs}) is assigned to the direct electron tunneling from Q_B^- to P^+ that occurs when $-\Delta G^\circ_{AB}$ is at least 60 meV more favorable than in wild type RCs. However, k_{BP}^{obs} can be slow for other reasons. In *Rb. sphaeroides*, RCs without an H

subunit k_{BP} is 0.01 s^{-1} (Debus et al. 1985). With the large changes in the L subunit, the H subunit could be lost. However, all three subunits were found with a Protein Chip Array (Ciphergen Biosystems, Inc) in the mutant RCs (data not shown) which is consistent with the earlier characterization of the protein (Coleman and Youvan 1993).

The back reaction ($k_{BP}{}^{obs}$) was monitored from the decay of the P^+ signal. This rate can also be slow if solution oxidants oxidize $Q_A{}^-$ or $Q_B{}^-$ trapping P^+ which then reacts slowly with solution reductants. However, several lines of evidence support the presence of a bound, reducible secondary quinone. First, the slow charge recombination as well as the ability of RCs to oxidize two cytochromes *c* ($D^{(1)}$ and $D^{(2)}$) are dependent on added UQ_4. Both assays provide the same K_d for UQ_4 at Q_B (Figure 7). In addition, the rate of reoxidation of P^+ is comparable to that identified with the direct electron transfer in *Rb. sphaeroides* and *Rb. capsulatus* L212,L213 double mutants supporting the same mechanism for charge recombination (Takahashi and Wraight 1990; Hanson et al. 1992; Takahashi and Wraight 1992; Maroti et al. 1994; Paddock et al. 1994). Lastly, the decay of the $P^+Q_B{}^-$ state is pH independent from 4.5 to 10.5. P^+ reduction or Q^- oxidation by solution donors or acceptors often depends on strongly pH dependent reactions. In contrast, the direct tunneling from $Q_B{}^-$ to P^+, with its small $-\Delta G^\circ_{AB}$ dependence, varies only weakly with pH (Labahn et al. 1994).

Despite the evidence that there is a secondary quinone, no stable $Q_B{}^-$ is observed when electron donor is added to trap $PQ_B{}^-$. In wild type RCs, the $Q_B{}^-$ state is stable for seconds after a single flash in the presence of an electron donor to reduce P^+. In contrast, in the mutant the semiquinone decays at $\approx$7 s^{-1}, a rate comparable to the rate at which the electron moves from $Q_A{}^-$ to Q_B. The decay of the semiquinone signal at 450 nm could be due to the formation of a protonated, neutral semiquinone Q_B (Lavergne et al. 1999). However, preliminary measurements did not show significant signal with a peak at 420 nm, a local maximum for Q^-H^+ absorption (Bensasson and Land 1973). In addition, the absence of proton uptake also argues against formation of the neutral semiquinone. However, the behavior in the A6D1 RCs is similar to that found in site-directed mutant RCs where no stable semiquinone or proton uptake is seen when electron transfer from $Q_A{}^-$ to Q_B (at $k_{AB}{}^{(1)}$) or to $Q_B{}^-$ (at $k_{AB}{}^{(2)}$) is very slow (Takahashi and Wraight 1990; Hanson et al. 1992; Maroti et al. 1994; Paddock et al. 1994).

The electron transfer rate from $Q_A{}^-$ to Q_B

There are two different electron transfer reactions from Q_A to the secondary quinone. In the first ($k_{AB}{}^{(1)}$) $Q_A{}^-$ reduces a neutral Q_B forming the anionic semiquinone. In the presence of electron donor the electron transfer from $Q_A{}^-$ to $Q_B{}^-$ ($k_{AB}{}^{(2)}$) is proceeded by an uphill proton transfer followed by electron transfer and binding a second proton to form QH_2 (Graige et al. 1996). The electron transfer from $Q_A{}^-$ to Q_B occurs faster than 10^4 s^{-1} in wild type *Rb. capsulatus*, *Rb. sphaeroides*, or *Rps. viridis* RCs (Baciou et al. 1993; Okamura and Feher 1995). At physiological pHs, this reaction is independent of pH. Above pH $\approx$9 the reaction slows as the pH is raised.

The A6D1 mutant behaves quite differently. Several lines of evidence show that for the mutant the electron transfer rate is only $\approx$10 s^{-1} not 10^4 s^{-1}. First, the quantum yield of RCs that form the $P^+Q_B{}^-$ state after each flash is only $\approx$50%, as expected if k_{AP}, the rate of the competing electron transfer from $Q_A{}^-$ to P^+, is similar to $k_{AB}{}^{(1)}$ (Figure 5). Second, the cytochrome c double flash measurement shows $Q_A{}^-$ is oxidized by Q_B at $\approx$14 s^{-1} (Figure 7). In addition, the steady state cytochrome *c* oxidation slows after the first quinone reduction (Figure 8) consistent with $k_{AB}{}^{(1)}$ being the rate determining step for the whole photocycle (Figure 1). The rate limiting step for electron transfer from $Q_A{}^-$ to Q_B in isolated wild type RCs is a process such as proton, protein, or cofactor (Stowell et al. 1997) motion (Graige et al. 1998) rather than the electron transfer itself. It is not known which process is slowed in the A6D1 RCs.

In single site-directed mutations in the Q_B site such as L213DN, $k_{AB}{}^{(1)}$ at pH 7–8 can be as slow as several hundred s^{-1}. However, analysis of the pH dependence shows that at low pH the rate is comparable to the 5000 s^{-1} found in wild-type RCs at pH 8 (Takahashi and Wraight 1992; Paddock et al. 1994). Thus, the transition to pH dependence is shifted from pH 9 to much lower pH's so that a slow rate is found at pH 7–8. In contrast, the pH dependence of the quantum yield of $P^+Q_B{}^-$ (Figure 5) suggests that $k_{AB}{}^{(1)}$ is relatively pH independent in the A6D1 mutant.

In the A6D1 mutant $k_{AB}{}^{(2)}$ was not measured directly. However, the cytochrome *c* reduction in steady state or individual turnovers suggests that $k_{AB}{}^{(2)}$ is not slower than $k_{AB}{}^{(1)}$. As $k_{AB}{}^{(1)}$ is very slow the second

reduction of Q_B could also be impaired. It is this step, where proton transfer is most closely coupled to electron transfer, that has previously been shown to be most sensitive to site-directed mutations in the Q_B site.

Conclusion

One of the goals of the sequence substitution mutation was to explore how the RCs ensure that the ubiquinones at Q_A and Q_B sites maintain their distinct functions (Coleman and Youvan 1993). However, despite the substitution of 42 residues from the Q_A site for 35 in the Q_B site, the A6D1 does not behave as if it has 2 Q_A's. There is still one quinone binding site with high affinity and one where the quinone affinity is comparable to that found Q_B in the wild type. The electron appears to reach the secondary quinone via Q_A^- rather than by direct electron transfer from P. The electron tunneling from Q_B^- to P^+ is much slower than from Q_A^- to P^+ as in wild type RCs. The A6D1 has some characteristics of the GluL212/AspL213 to Ala/Ala double mutant (Hanson et al. 1992; Maroti et al. 1994). These important acidic residues near Q_B are also modified in the A6D1 mutant. However, the major difference from previously studied mutants that change individual residues is that in A6D1 RCs the first electron transfer from Q_A^- to Q_B ($k_{AB}^{(1)}$) is very slow and apparently independent of pH. In most other mutants $k_{AB}^{(1)}$ is fast at low pH, but may slow at higher pH. While the electron transfer from Q_A^- to Q_B^- ($k_{AB}^{(2)}$) has not been measured, steady state cytochrome c oxidation rates suggests that it is not slower than $k_{AB}^{(1)}$. In previously studied site directed mutants $k_{AB}^{(2)}$ is the rate that is most sensitive to mutations in the Q_B site.

Acknowledgements

We are grateful Mel Okamura for insightful comments and Dr Ma Sha for carrying out the protein chip analysis of the A6D1 RCs. We would like to acknowledge the financial support of the Department of Agriculture CSREES 1999-01256 (to MRG) and the Department of Energy Division of Energy Biosciences 99ER20211 (to DCY) and N.I.H. RR03060 for maintenance of central facilities at City College.

References

Allen JP, Williams JC, Graige M, Paddock M L, Labahn A, Feher G and Okamura MY (1998) Free energy dependence of the direct charge recombination from the primary and secondary quinones in reaction centers from *Rhodobacter sphaeroides*. Photosynth Res 55: 227–233

Baciou L, Bylina EJ and Sebban P (1993) Study of wild type and genetically modified reaction centers from *Rhodobacter capsulatus*. Structural comparison with *Rhodopseudomonas viridis* and *Rhodobacter sphaeroides*. Biophysical J 65: 652–660

Bensasson R and Land EJ (1973) Optical and kinetic properties of semireduced plastoquinone and ubiquinone: Electron acceptors in photosynthesis. Biochim Biophys Acta 176–181

Bylina EJ and Youvan DC (1987) Genetic engineering of herbicide resistance: Saturation mutagenesis of isoleucine 229 of the reaction center L subunit. Z Naturforsch 42c: 769–774

Coleman WJ and Youvan DC (1990) Spectroscopic analysis of genetically modified photosynthetic reaction centers. Ann Rev Biophys Biophysical Chem 19: 333–367

Coleman WJ and Youvan DC (1993) Actavistic reaction centre. Nature 366: 517–518.

Debus RJ, Feher G and Okamura MY (1985) LM complex of reaction centers from *Rhodopseudomonas sphaeroides* R-26: Characterization and reconstitution with the H subunit. Biochemistry 24: 2488–2500

Deisenhofer J and Michel H (1991) High-resolution structures of photosynthetic reaction centers. Annu Rev Biophys Chem 20: 247–266

Graige MS, Feher G and Okamura MY (1998) Conformational gating of the electron transfer reaction $Q_A^-Q_B \rightarrow Q_AQ_B^-$ in bacterial reaction centers of *Rhodobacter sphaeroides* determined by a driving force assay. Proc Natl Acad Sci USA 95: 11679–11684

Graige MS, Paddock ML, Bruce JM, Feher G and Okamura MY (1996) Mechanism of proton-coupled electron transfer for quinone (Q_B) reduction in reaction centers of *Rb. Sphaeroides*. J Am Chem Soc 118: 9005–9016

Gunner, MR and Dutton PL (1989) Temperature and -ΔG dependence of the electron transfer from BPh^- to Q_A in reaction center protein from *Rhodobacter sphaeroides* with different quinones as Q_A. J Am Chem Soc 111: 3400–3412

Gunner MR, Tiede DM, Prince RC and Dutton PL (1982) Quinones as prosthetic groups in membrane electron-transfer proteins I: Systematic replacement of the primary ubiquinone of photochemical reaction centers with other quinones In: Trumpower BL (ed) Function of Quinones in Energy Conserving Systems, pp 265–269, Academic Press, New York

Hanson DK, Baciou L, Tiede DM, Nance M, Schiffer M and Sebban P (1992) In bacterial reaction centers protons can diffuse to the secondary quinone by alternative pathways. Biochim Biophys Acta 1102: 260–265

Hutchens TW and Yip T-T (1993) New desorption strategies for the mass spectrometric analysis of macromolecules. Rapid Commun Mass Spectrom 7: 576

Kabsch W and Sander C (1983) Dictionary of protein secondary structure: Pattern recognition of hydrogen-bonded and geometrical features. Biopolymers 22: 2577–2637.

Kleinfeld D, Okamura MY and Feher G (1984) Electron transfer in reaction centers of *Rhodopseudomonas sphaeroides*: I. Determination of the charge recombination pathway of $D^+Q_AQ_B^-$ and free energy and kinetic relations between $Q_A^-Q_B$ and $Q_AQ_B^-$. Biochim Biophys Acta 766: 126–140

Komiya H, Yeates TO, Rees DC, Allen JP and Feher G (1988) Structure of the reaction center from *Rhodobacter sphaeroides* R-26 and 2.41: Symmetry relations and sequence comparisons between different species. Proc. Natl Acad Sci USA 85: 9012–9016

Labahn A, Bruce JM, Okamura MY and Feher G (1995) Direct charge recombination from $D^+Q_AQ_B^-$ to DQ_AQ_B in bacterial reaction centers from *Rhodobacter sphaeroides* containing low potential quinone in the Q_A site. Chem Phys 97: 355–366

Labahn A, Paddock ML, McPherson PH, Okamura MY and Feher G (1994) Direct charge recombination from $D^+Q_AQ_B^-$ to DQ_AQ_B in bacterial reaction centers from *Rhodobacter sphaeroides*. J Phys Chem 98: 3417–3423

Lancaster CRD, Ermler U and Michel H (1995) The structures of photosynthetic reaction centers from purple bacteria as revealed by x-ray crystallography. In: Blankenship RE, Madigan MT and Bauer CE (ed) Anoxygenic Photosynthetic Bacteria, pp 503–526. Kluwer Academic Publishers, Dordrecht, The Netherlands

Lavergne J, Matthews C and Ginet N (1999) Electron and proton transfer on the acceptor side of the reaction center in chromatophores of *Rhodobacter capsulatus*: Evidence for direct protonation of the semiquinone state of Q_B. Biochemistry. 38: 4542–4552

Mancino LJ, Dean DP and Blankenship RE (1984) Kinetics and thermodynamics of the $P870^+Q_A^- \rightarrow P870^+Q_B^-$ reaction in isolated reaction centers from the photosynthetic bacterium *Rhodopseudomonas sphaeroides*. Biochim Biophys Acta 764: 46–54

Maroti P and Wraight CA (1988) Flash-induced H^+ binding by bacterial photosynthetic reaction centers: Influences of the redox states of the acceptor quinones and primary donor. Biochim Biophys Acta 934: 329–347

Maroti P, Hanson DK, Baciou L, Schiffer M and Sebban P (1994) Proton conduction within the reaction centers of *Rhodobacter capsulatus*: The electrostatic role of the protein. Proc Natl Acac Sci 91: 5617–5621

McPherson PH, Okamura MY and Feher G (1993) Light-induced proton uptake by photosynthetic reaction centers from *Rhodobacter sphaeroides* R-26.1. II. Protonation of the state $DQ_AQ_B^{2-}$. Biochim Biophys Acta 1144: 309–324

Okamura MY and Feher G (1995) Proton-coupled electron transfer reactions of Q_B in reaction centers from photosynthetic bacteria In: Blankenship R, Madigan M and Bauer C (eds) Anoxygenic Photosynthetic Bacteria, pp 577–593. Kluwer Academic Publishers, Dordrecht, The Netherlands

Paddock ML, Rongey SH, Feher G and Okamura MY (1989) Pathway of proton transfer in bacterial reaction centers: Replacement of glutamic acid 212 in the L subunit by glutamine inhibits quinone (secondary acceptor) turnover. Proc Natl Acad Sci USA 86: 6602–6606

Paddock ML, McPherson PH, Feher G and Okamura MY (1990) Pathway of proton transfer in bacterial reaction centers: Replacement of serine-L223 by alanine inhibits electron and proton transfers associated with reduction of quinone to dihydroquinone. Proc Natl Acad Sci 87: 6803–6807

Paddock ML, Rongey SH, McPherson PH, Juth A, Feher G and Okamura MY (1994) Pathway of proton transfer in bacterial reaction centers: Role of Aspartate-L213 in proton transfers associated with reduction of quinone to dihydroquinone. Biochemistry. 33: 734–745

Paddock ML, Feher G and Okamura MY (1997) Proton and electron transfer to the secondary quinone (Q_B) in bacterial centers: The effect of changing the electrostatics in the vicinity of Q_B by interchanging Asp and Glu at the L212 and L213 sites. Biochemistry. 36: 14238–14249

Parson WW (1969) The reaction between primary and secondary electron acceptor in bacterial photosynthesis. Biochim Biophys Acta 189: 384–396

Prince RC and Youvan DC (1987) Isolation and spectroscopic properties of photochemical reaction centers from *Rhodobacter capsulatus*. Biochim Biophys Acta 890: 286–291

Stowell MHB, McPhillips TM, Rees DC, Soltis SM, Abresch E and Feher G (1997) Light-induced structural changes in photosynthetic reaction center: Implications for mechanism of electron-proton transfer. Science. 276: 812–816

Takahashi E and Wraight CA (1990) A crucial role for Asp^{L213} in the proton transfer pathway to the secondary quinone of reaction centers from *Rhodobacter sphaeroides*. Biochim Biophys Acta 1020: 107–111

Takahashi E and Wraight CA (1992) Proton and electron transfer in the acceptor quinone complex of *Rhodobacter sphaeroides* reaction centers: Characterization of site-directed mutants of the two ionizable residues, Glu L212 and Asp L213, in the Q_B binding site. Biochemistry 31: 855–866

Takahashi E and Wraight CA (1994) Molecular genetic manipulation and characterization of mutant photosynthetic reaction centers from purple nonsulfur bacteria. Advances in Molecular and Cell Biology 10: 197–251

Williams JC, Steiner LA and Feher G (1986) Primary structure of the reaction center from *Rhodopseudomonas sphaeroides*. Proteins 1: 312-325

Woodbury NW, Parson WW, Gunner MR, Prince RC and Dutton PL (1986) Radical-pair energetics and decay mechanisms in reaction center containing anthraquinones or benzoquinones in place of ubiquinone. Biochim Biophys Acta 851: 6–22

Wraight CA (1977) Electron acceptor of photosynthetic bacterial reaction centers. Direct observation of oscillatory behavior suggesting two closely equivalent ubiquinones. Biochim. Biophys Acta 495: 525–531

Wraight CA and Clayton RK (1973) The absolute quantum efficiency of bacteriochlorophyll photoxidation in reaction centers. Biochim Biophys Acta 333: 246–260

Wraight CA and Stein RR (1980) Redox equilibrium in the acceptor quinone complex of isolated reaction centers and the mode of action of o-phenanthroline. FEBS Letts 113: 73–77

Wraight CA and Stein RR (1983) Bacterial reaction centers as a model for photosystem II: Turn over of the secondary acceptor quinone In: Inoue Y, Crofts AR, Govindjee, Murata N, Renger G and Satoh K (eds) The Oxygen Evolving System of Photosynthesis, pp 383–393. Academic, New York